1 **Supplementary information: Flow-through stable isotope probing (Flow-SIP) minimizes**

2 **cross-feeding in complex microbial communities**

3

4 **Supplementary text**

5 **Materials and experimental setup**

6 Schemes of the incubation setup of recirculated and flow-through approaches are shown in Figure 1.

7 For the flow-through approach, the screw caps of the medium reservoir and the waste collection bottle

8 were equipped with two ports, one for the tubing inlet and one for sterile pressure equalization using

9 a membrane filter (0.2 µm). For the recirculated approach, a small bottle was used as medium reservoir

10 with two ports, from which medium was withdrawn and recirculated back, respectively. For both

11 approaches, the medium reservoir was connected to the top of the filter holder (stainless steel, 47

12 mm, Sartorius) and a peristaltic pump was placed after the filter holder. To open and close the filter

13 holder as well as to remove aliquots of the medium for chemical analysis during the incubation, a

14 three-way valve was connected to the bottom of the filter holder. Material used for both recirculated

15 and flow-through approaches are given in Table S1. All material except for the three-way-valves was

16 sterilized by autoclaving, three-way valves were sterilized by rinsing in 70% ethanol and autoclaved

17 distilled water. Mineral medium was prepared according to Palatinszky *et al.* [1], with some

18 modifications: instead of 4 g L^{-1} CaCO$_3$, we used 0.01 g L^{-1} (1 mM, as a calcium source), and, as substrate

19 for autotrophic C-fixation, we added ^{13}C-NaHCO$_3$ (98 atom%) with a final concentration of 2 mM,

20 resulting in a final ^{13}C-labelling percentage of approximately 66 atom%. For batch and recirculated

21 incubations, 20 ml of medium were inoculated. We accounted for the dead volume of the filter holder

22 and tubing (9 ml) and thus only 11 ml medium were added to the medium reservoir of the recirculated

23 approach. In the flow-through incubations, approximately 624 ml of medium were supplied over 24 h

24 (i.e., flow rate of 26 mL h^{-1}).

25 Activated sludge was sampled from the nitrification basin of the municipal wastewater treatment plant

26 Aalborg West (luftningstanke, Renseanlæg Vest), Denmark, on March 16th and 18th, 2016. Sludge was

27 disrupted by sonication to yield single cells or colonies to reduce diffusive cross-feeding due to the

28 large 3D-structure of the flocs. 20 ml aliquots of sludge (diluted 1:5 in mineral medium) were sonicated

29 on ice for 120 s using 20% power and 1x cycle settings (Bandelin HD2200, probe MS73), and were

30 allowed to settle for 10 min. The top 15 ml of the sludge suspensions, containing smaller flocs or single

31 colonies and cells, were filtered through 20 µm nylon mesh membrane filters (Magna, Fisher Scientific)

32 to remove residual large flocs. To remove residual substrates from the filtrate, cells were pelleted by

33 centrifugation (20 min, 10°C, 4 200 g), supernatant was discarded, and cells were gently resuspended

34 in mineral medium with ^{12}C-NaHCO$_3$ and without ammonium. To avoid the use of storage compounds

35 during the incubation, cells were exposed to a starvation period of approximately 8 - 10 h before start

36 of the incubation. To determine optimal cell density for the incubations, different volumes of

37 sonicated, washed cells were filtered onto 0.2 µm filters, stained by DAPI and inspected by an

38 epifluorescence microscope.

39 Under sterile conditions, support filters (for E1, glass fibre filters, Advantec, GC50, 47mm, and for E2

40 nylon membrane filters Magna, Fisher Scientific, 47mm) and membrane filters (0.2µm polycarbonate,

41 Nucleopore Whatman 47mm) were placed into filter holders (backpressure grids were omitted) fitted

42 with a valve at the filter holder outlet. Filter holders were then filled bubble-free with mineral medium

43 and closed off until cells were applied onto the filter membrane. Using syringes, sonicated, starved

44 cells were gently filtered onto the membranes, discarding the flow-through. To ensure even settling of

45 cells on the membrane surface, additional 20 ml mineral medium (with ^{12}C-NaHCO$_3$ and without

46 ammonium) were gently pushed through the filter holder, discarding the flow-through. Shortly before

47 the start of the incubation, the medium in the filter holder was replaced by medium containing ^{13}C-

48 NaHCO$_3$ (but no ammonium). Filter holders were then connected to sterile tubing of the incubation

49 setup (Figure 1). The same amount of biomass as in the recirculated and flow-through incubations

50 were added to the batch incubations. At the start of the incubation, ammonium was added from a

51 stock solution to batch incubation bottles and into the medium reservoir and fresh medium bottle of

52 the recirculated and flow-through approaches, respectively. Incubations were done in the dark for 24h

53 at *in situ* temperature of the nitrification basin in Aalborg Vest (14°C). Immediately after the setup of

54 the incubation, and after approximately 12, 18 and 24 h, subsamples were collected for concentration

55 measurements of ammonium, nitrite and nitrate. In both flow-through and recirculated incubations,

56 samples were collected at the filter holder outlet, and from batch incubations, bulk samples were

57 collected, and cells were removed by centrifugation. Samples were stored at -20°C until analysis.

58 At the end of the incubation, filter holders were closed off using the valve at the filter outlet,

59 disconnected from the tubing, and cells on the membrane filter inside the filter holders were fixed

60 with formaldehyde (3% formaldehyde in 1x phosphate buffered saline; PBS). To avoid disturbing the

61 cells' position on the membrane filter, 20 ml formaldehyde solution were gently pushed through the

62 filter holders, thereby replacing medium. Filter holders were then closed using the valve connected at

63 the filter holder outlet and incubated for 30 min at room temperature. Formaldehyde was removed

64 by pushing 20 ml 1x PBS through the filter holder, followed by 20 ml distilled water. After pushing out

65 all liquid, filter holders were disassembled, and membrane filters were air-dried and frozen at -20°C

66 until FISH and nanoSIMS analyses. Batch incubation samples were also filtered on a membrane filter,

67 fixed and stored the same way as the flow-through and recirculated samples.

68   Nitrification activity was monitored by ammonium consumption, and nitrite and nitrate production.

69 Ammonium, nitrite and nitrate concentrations were quantified after 0, 12, 18 and 24 h by a

70 colorimetric procedure as described in Hood-Nowotny *et al.* [2] and Garcia-Robledo *et al.* [3].

71 **FISH and nanoSIMS analyses**

72 In addition to cells fixed after incubation, bulk activated sludge samples were fixed with formaldehyde

73 as previously described [4]. These samples were used to screen for presence of nitrifier populations by

74 FISH using probes for AOB (probes NEU, [5]; Nso1225, [6]; Nmv/Ncmob [7]; Ncom1025, [8]; Cl6a192,

75 [9]) and NOB (Nit3, [5]; Ntspa1431 and Ntspa1151, [10]; Ntoga122, [11]). We detected AOB

76 populations related to *Nitrosomonas oligotropha* (targeted by probe Cl6a192) and *Nitrosomonas*

77 *eutropha/europea/urea* (targeted by probe NEU). We further detected *Nitrotoga*-affiliated NOB and

78   lineage 1 and 2 *Nitrospira* (targeted by probe Ntspa 1431 and 1151, respectively). Previous

79   metagenomic analyses showed that WWTP Aalborg West does not harbor comammox *Nitrospira* [12,

80   13], whose presence would have confounded the results of our study, as comammox *Nitrospira* are

81   able to oxidize ammonia but are not distinguishable from the canonical lineage 2 *Nitrospira* by FISH.

82   For all combined FISH and nanoSIMS analyses, we used probe mixes for AOB (Cl6a192 and NEU) and

83   NOB (Ntoga122, Ntspa1431 and Ntspa1151).

84   Before FISH analysis, laser markings were made on membrane filters using a laser microdissection

85   microscope (Leica LMD 7000, Germany). FISH on sections of the incubated filters was done as

86   previously described by Daims [4]. All FISH probes were double labelled with FitC (AOB in E1; NOB in

87   E2), Cy3 (NOB in E1), or Cy5 (AOB in E2) fluorophores [14]. We observed strong non-specific binding of

88   the fluorophores, especially of Cy3 and Cy5, to the membrane filter surface. This non-specific binding

89   was overcome by using CARD-FISH hybridization buffer [15] instead of normal FISH hybridization buffer

90   in hybridizations of E1 samples. Filter sections of E2 were pre-incubated in 1:10 diluted blocking

91   reagent before hybridization [15]. After FISH, cells were counterstained with DAPI before fluorescent

92   images were acquired on a confocal laser scanning microscope (SP7, Leica, Germany, equipped with a

93   white light laser).

94   For nanoSIMS analyses, selected filter sections were attached to antimony-doped silicon wafer

95   platelets (7.1 x 7.1 x 0.11 mm, Active Business Company, Brunnthal, Germany) by a commercially

96   available superglue (Loctide®, Henkel, Ireland), and coated with AuPd thin films (30 nm nominal

97   thickness) using a sputter coater (K550X Emitech, Quorum Technologies Ltd., Ashford, UK). In the flow-

98   through incubations, a thin, yellow layer of salt crystals was formed on the filter membranes, which

99   strongly reduced the conductivity of the sample surfaces upon sputtering with AuPd. To remove this

100   layer prior to AuPd coating, we tested washing the filter membrane sections from experiment E2, flow-

101   through incubation in either 1N HCl or 1N HNO_3 for 10 min. Both acid treatments successfully removed

102   the yellow layer and rendered the samples sufficiently conductive for nanoSIMS analyses. We

103   subsequently used HCl for washing all other samples. After acid treatment, samples were rinsed with

104   water (Milli-Q, >18.2 MOhm, Millipore) and 70% ethanol. For maintaining comparability and to remove

105   possible ^{13}C-bicarbonate contamination, samples on filter membranes from batch and recirculated

106   incubations were also washed with 1N HCl in the same way.

107   NanoSIMS measurements were performed on a NanoSIMS 50L (Cameca, Gennevilliers, France) at the

108   Large-Instrument Facility for Environmental and Isotope Mass Spectrometry at the University of

109   Vienna. Prior to data acquisition, analysis areas were pre-sputtered utilizing a high-intensity, slightly

110   defocused Cs^+ ion beam (400 pA beam current, ~1,5 μm spot size). Data were acquired as multilayer

111   image stacks by sequential scanning of a finely focused Cs^+ primary ion beam (approximately 80 nm

112   probe size at 2 pA beam current) over areas between 36×36 and 74×74 μm^2 at 512×512 pixel image

113   resolution and a primary ion beam dwell time of 5 to 10 ms/(pixel∗cycle). The detectors were

114   positioned to enable parallel detection of $^{12}C_2^-$, $^{12}C^{13}C^-$, $^{12}C^{14}N^-$, $^{31}P^-$ and $^{32}S^-$ secondary ions and the mass

115   spectrometer was tuned to achieve a mass resolving power (MRP) of >9 000 (according to Cameca's

116   definition) for detection of C_2^- and CN^- secondary ions, respectively.

117   NanoSIMS images were processed using the software WinImage version 2.0.8 (Cameca, France). Prior

118   to stack accumulation, the individual images were aligned to compensate for positional variations

119   arising from primary ion beam and/or sample stage drift. Secondary ion signal intensities were dead

120   time corrected on a per-pixel basis. C isotope composition images displaying the $^{13}C/(^{12}C+^{13}C)$ isotope

121   fraction, designated as ^{13}C atom%, were inferred from the C_2^- secondary ion signal intensity

122   distribution images via per-pixel calculation of $^{13}C^{12}C^-/(2 \cdot ^{12}C_2^- + ^{13}C^{12}C^-)$ intensity ratios.

123   Regions of interest (ROIs), referring to individual cells, were manually defined utilizing the nitrogen-,

124   phosphorus- and sulfur-related secondary ion signal intensity distribution maps as indicators of

125   biomass and the respective FISH image. These ROIs were cross-checked by the

126   topographical/morphological appearance of the sampled areas in secondary electron intensity

127   distribution images that were recorded simultaneously with the secondary ion images. Statistical

128   significance of the difference of the ^{13}C-enrichment between groups within each approach was

129   analyzed by the Kruskal-Wallis test followed by a non-parametric multiple comparison test (Dunn's

130   test), using the R package "dunn.test" [16].

Nitrite diffusion model

In order to determine nitrite distributions surrounding the AOB colonies and to quantify the potential exchange rates with NOB colonies, the flow-condition around a single AOB colony on the Flow-SIP filter was simulated.

The steady-state Navier-Stokes equations are given by:

$$\rho(\boldsymbol{u} \cdot \nabla)\boldsymbol{u} = -\nabla p + \mu \nabla^2 \mathbf{u}$$

With the continuity equation for incompressible fluids:

$$\nabla \cdot \boldsymbol{u} = 0,$$

where ρ is the density, ∇ is the del operator, μ the dynamic viscosity of water, p the pressure and $\boldsymbol{u}$ the velocity vector. The time-dependent advection-diffusion equation is given by:

$$\frac{\partial C}{\partial t} = -D\nabla^2 C + \boldsymbol{u} \cdot \nabla C,$$

where C is the nitrite concentration and $D = 1.7 \cdot 10^{-9}$ m^2 s^{-1} is the isotropic diffusion of nitrite. The equations were solved in the COMSOL Multiphysics® software.

Simulating the full 3-dimensional complexity as found on the Flow-SIP filter is numerically expensive and requires precise information about the cell and colony structures. Therefore, certain assumptions were made when generating the model domain. First, it is assumed that the AOB colonies are of spherical shape with a radius that can be estimated from measured volumes. For AOB colonies exceeding 50 cells, it was shown that the colony volume can be empirically described using: $V_{col} = n_{cell}^{1.56} e^{-3.28}$, where n$_{cell}$ is the cell number [17]. For colonies with fewer cells no empirical relation exists. Therefore, the volume for 50 cells was linearly scaled down to a theoretical volume of a single

157 cell multiplied with the cell number: $V_{col} = \frac{50^{0.56}e^{-3.28}}{50} \cdot n_{cell}$, which is valid for 1-50 cells. Finally, within

158 the domain the reactive, spherical AOB colony was centered in a cylinder. To minimize wall-effects,

159 the radius of the cylinder was adjusted to 120 µm, which is more than 20 times the radius of the AOB

160 colony.

161 To mimic conditions of the experimental setup, a symmetric outer boundary with a constant inlet flow

162 velocity U_0 and a no-slip boundary condition along the colony's surface was assumed. The inflow

163 nitrite-concentration was adjusted to 0 µmol l^{-1}. To simulate the nitrite production of the AOB colonies,

164 a constant normal flux (J_n) was imposed at the surface of the colony, which was calculated based on

165 the cell specific volumetric rates and normalized to the surface area:

166

167
$$J_n = \frac{n_{cell} \cdot R_{cell}}{S_{col}}$$

168

169 With a cell specific volumetric rate of $R_{cell} = 2.6$ fmol cell^{-1}h^{-1} [17–20] and a surface area of $S_{col} =$

170 $4\pi r_{col}^2$. The described approach reduces the decisive parameters to cell numbers and flow velocity.

171 In more than 200 stationary model runs ($\frac{dC}{dt} = 0$), cell numbers were varied between $n_{cell} =$

172 $5, 50, 500$ cells and the imposed flow velocity was sequentially increased from U_0 = 0.1 - 100 µm s^{-1} in

173 1.25 µm s^{-1} steps.

174 Post-processing was performed in Matlab (Mathworks 2017b). Briefly, nitrite concentrations were

175 extracted along the equator up to a distance of 100 µm of the colony surface. This procedure was

176 repeated for all imposed flow velocities and subsequently interpolated to an equidistant grid.

177 Subsequently, contour lines were extracted.

178 Additionally, time-dependent nitrite accumulation around AOB colonies without flow ($\mathbf{u} = 0$), i.e. in a

179 diffusion-controlled system, were simulated in the same domain as described above. After a simulation

180 time of 24 hours, nitrite profiles along the equator were extracted for 5, 50 and 500 cells (Figure S2).

181 **Supplementary references**

182 1. Palatinszky M, Herbold C, Jehmlich N, Pogoda M, Han P, Bergen M Von, et al. Cyanate as an

183 energy source for nitrifiers. *Nature* 2015; **524**: 105–108.

184 2. Hood-Nowotny R, Umana NH-N, Inselbacher E, Oswald- Lachouani P, Wanek W. Alternative

185 Methods for Measuring Inorganic, Organic, and Total Dissolved Nitrogen in Soil. *Soil Sci Soc Am*

186 *J* 2010; **74**: 1018.

187 3. García-Robledo E, Corzo A, Papaspyrou S. A fast and direct spectrophotometric method for the

188 sequential determination of nitrate and nitrite at low concentrations in small volumes. *Mar*

189 *Chem* 2014; **162**: 30–36.

190 4. Daims H. Use of fluorescence *in situ* hybridization and the daime image analysis program for

191 the cultivation-independent quantification of microorganisms in environmental and medical

192 samples. *Cold Spring Harb Protoc* 2009; **4**: 1–7.

193 5. Wagner M, Rath G, Amann R, Koops H-P, Schleifer K-H. *In situ* Identification of Ammonia-

194 oxidizing Bacteria. *Syst Appl Microbiol* 1995; **18**: 251–264.

195 6. Mobarry B, Wagner M, Urbain V, Rittmann BE, Stahl D a. Phylogenetic probes for analyzing

196 abundance and spatial organization of nitrifying bacteria. *Appl Environ Microbiol* 1996; **62**:

197 2156–2162.

198 7. Pommerening-Röser A, Rath G, Koops H-P. Phylogenetic Diversity within the Genus

199 *Nitrosomonas*. *Syst Appl Microbiol* 1996; **19**: 344–351.

200 8. Juretschko S. Mikrobielle Populationsstruktur und -dynamik in einer

201 nitrifizierenden/denitrifizierenden Belebtschlammanlage. 2000. Technische Universität

202 München.

203 9. Adamczyk J, Hesselsoe M, Iversen N, Horn M, Lehner A, Nielsen PH, et al. The Isotope Array, a

204 New Tool That Employs Substrate-Mediated Labeling of rRNA for Determination of Microbial

205 Community Structure and Function. *Appl Environ Microbiol* 2003; **69**: 6875–6887.

206 10. Maixner F, Noguera DRD, Anneser B, Stoecker K, Wegl G, Wagner M, et al. Nitrite concentration

207   influences the population structure of *Nitrospira*-like bacteria. *Environ Microbiol* 2006; **8**: 1487–

208   1495.

209   11.   Lücker S, Schwarz J, Gruber-Dorninger C, Spieck E, Wagner M, Daims H. *Nitrotoga*-like bacteria

210   are previously unrecognized key nitrite oxidizers in full-scale wastewater treatment plants.

211   *ISME J* 2015; **9**: 708–720.

212   12.   Albertsen M, Hansen LBS, Saunders AM, Nielsen PH, Nielsen KL. A metagenome of a full-scale

213   microbial community carrying out enhanced biological phosphorus removal. *ISME J* 2012; **6**:

214   1094–1106.

215   13.   Munck C, Albertsen M, Telke A, Ellabaan M, Nielsen PH, Sommer MOA. Limited dissemination

216   of the wastewater treatment plant core resistome. *Nat Commun* 2015; **6**: 8452.

217   14.   Stoecker K, Dorninger C, Daims H, Wagner M. Double labeling of oligonucleotide probes for

218   fluorescence *in situ* hybridization (DOPE-FISH) improves signal intensity and increases rRNA

219   accessibility. *Appl Environ Microbiol* 2010; **76**: 922–6.

220   15.   Pernthaler A, Pernthaler J, Amann R. Sensitive multi-color fluorescence *in situ* hybridization for

221   the identification of environmental microorganisms. In: Kowalchuk G, de Bruijn FJ, Head IM,

222   Akkermans ADL, van Elsas JD (eds). *Molecular Microbial Ecology Manual*, 2nd ed. 2004. Kluwer

223   Academic Publishers, Dordrecht, Boston, London, pp 711–726.

224   16.   Dinno A. dunn.test: Dunn's Test of Multiple Comparisons Using Rank Sums. R package version

225   1.3.2. http://CRAN.R-project.org/package=dunn.test. 2007.

226   17.   Coskuner G, Ballinger SJ, Davenport RJ, Pickering RL, Solera R, Head IM, et al. Agreement

227   between Theory and Measurement in Quantification of Ammonia-Oxidizing Bacteria. *Appl*

228   *Environ Microbiol* 2005; **71**: 6325–6334.

229   18.   Laanbroek HJ, Bodelier PLE, Gerards S. Oxygen consumption kinetics of *Nitrosomonas europaea*

230   and *Nitrobacter hamburgensis* grown in mixed continuous cultures at different oxygen

231   concentrations. *Arch Microbiol* 1994; **161**: 156–162.

232   19.   Daims H, Ramsing NB, Schleifer K, Wagner M. Cultivation-Independent, Semiautomatic

233 Determination of Absolute Bacterial Cell Numbers in Environmental Samples by Fluorescence

234 *In Situ* Hybridization. *Appl Environ Microbiol* 2001; **67**: 5810–5818.

235 20. Stieglmeier M, Mooshammer M, Kitzler B, Wanek W, Zechmeister-Boltenstern S, Richter A, et

236 al. Aerobic nitrous oxide production through N-nitrosating hybrid formation in ammonia-

237 oxidizing archaea. *ISME J* 2014; **8**: 1135–1146.

238

Supplementary figures

240

241
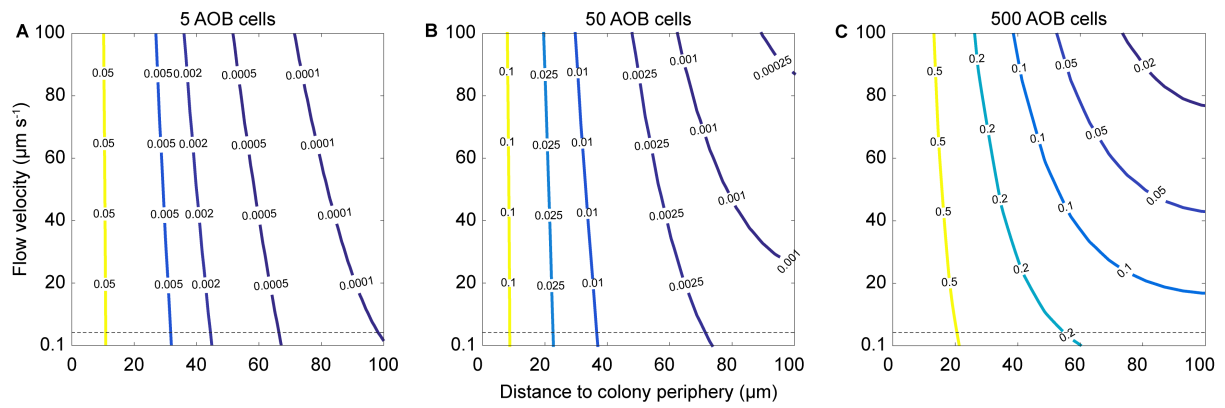
Figure S1. Nitrite diffusion model showing spatial distribution of nitrite concentrations (µM) around AOB colonies on the membrane filter in the flow-through approach, considering different flow velocities from 0.1 – 100 µm s^{-1}. The flow rate of 26 ml h^{-1} used in our experiment corresponds to a flow velocity of 4.2 µm s^{-1} (horizontal dashed grey line). The model was run for three different AOB colony sizes, consisting of either (A) 5, (B) 50 or (C) 500 cells. We analyzed AOB colonies ranging from single cell to approximately 250 cells in our experiments. The distance to the periphery of an AOB colony of 0 – 100 µm corresponds approximately to the distances between AOB and NOB colonies that we have observed. The contour lines represent nitrite concentration (µM).

250

251
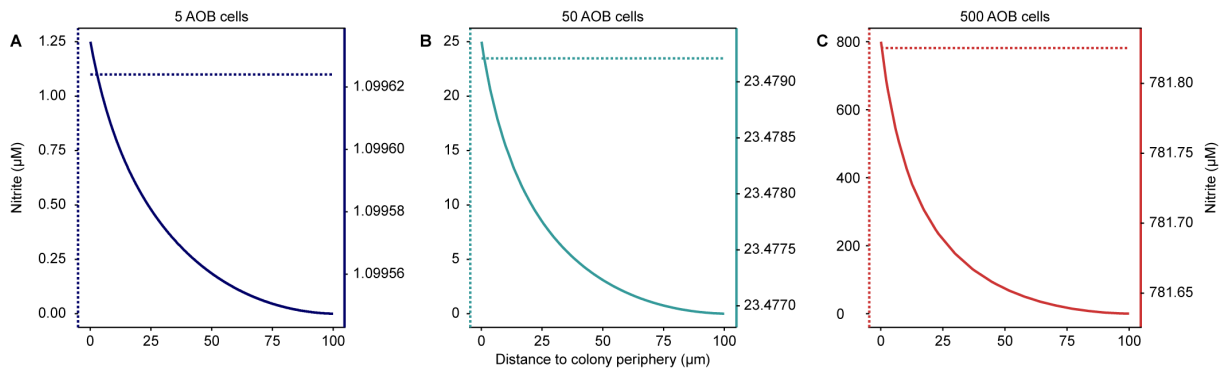
Figure S2. Spatial distribution of nitrite concentrations (μM) in absence of any flow surrounding AOB

colonies after 24h of incubation. The model was run for three different AOB colony sizes, consisting of

either (A) 5, (B) 50 or (C) 500 cells. Note the different scales on the y-axes – the solid lines (right y-axis)

were added to depict very minor changes in nitrite concentrations with distance to the AOB colony

peripheries (solid lines). At distances of 0-100 μm, modeled nitrite concentrations around AOB colonies

were very stable. Specifically, predicted nitrite concentrations over this distance around AOB colonies

consisting of 5 cells were approx. 1.1 μM, around AOB colonies of 50 cells 23 μM, and around AOB

colonies of 500 cells 780 μM after 24 h, as depicted by the dotted lines.
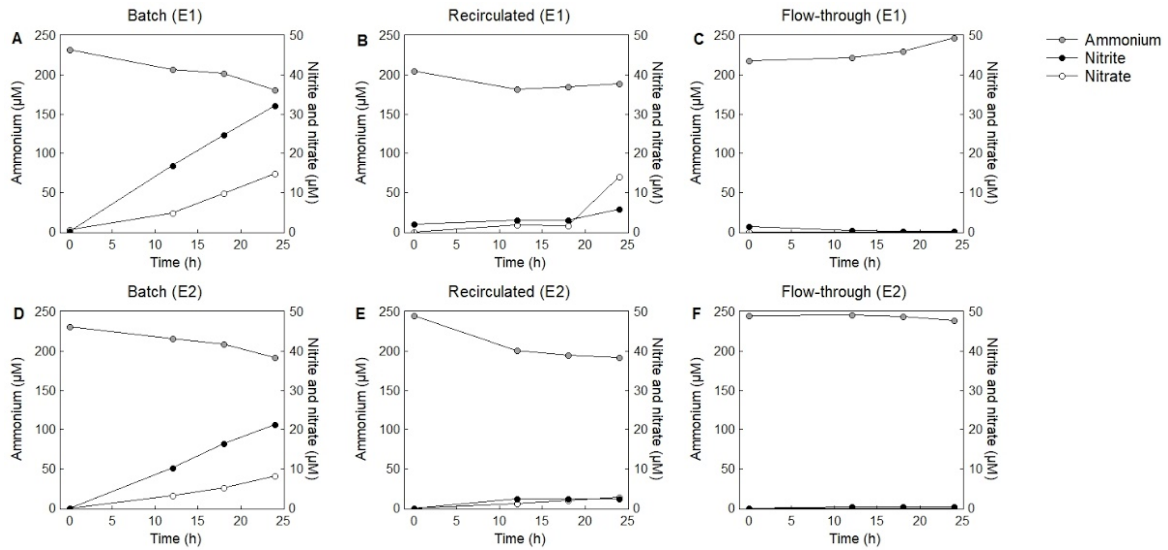
Figure S3. Nitrification activity in batch, recirculated and flow-through incubations of E1 (A-C) and E2 (D-F). Nitrification activity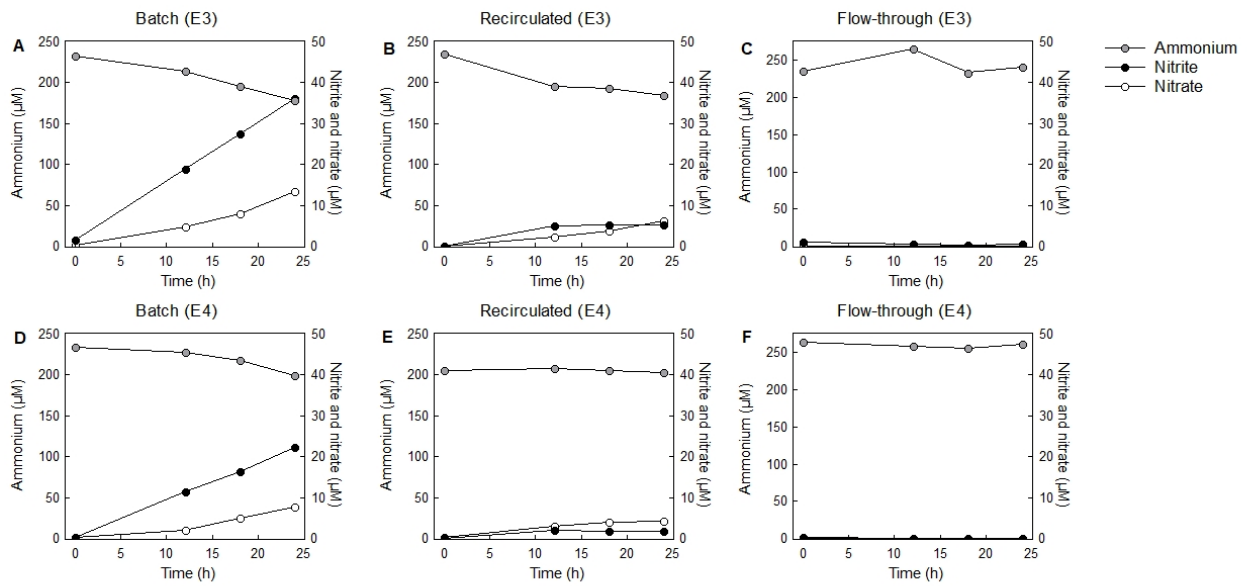 was monitored over the course of the incubation by ammonium consumption, and nitrite and nitrate production. Note that the drop in the ammonium concentration in the recirculated treatment between 0 and 12h was not due to ammonium consumption, but due to dilution by ammonium-free medium that was present in the tubing and filter holder at the beginning of the incubation. Nitrite and nitrate were not detectable in the flow-through incubation due to the strong dilution by the constant medium supply.

268

269 **Figure S4.** Nitrification activity in batch, recirculated and flow-through incubations of two additional

270 experiments (E3 and E4) to further support reproducibility of the Flow-SIP method. Nitrification activity

271 was monitored over the course of the incubation by ammonium consumption, and nitrite and nitrate

272 production. Note that the drop in the ammonium concentration in the recirculated treatment between

273 0 and 12h was not due to ammonium consumption, but due to dilution by ammonium-free medium

274 that was present in the tubing and filter holder at the beginning of the incubation. Nitrite and nitrate

275 were not detectable in the flow-through incubation due to the strong dilution by the constant medium

276 supply.

277   **Supplementary tables**

278   **Table S1.** Material used in flow-through and recirculated approaches. Schemes of the setup of both

279   approaches are given in Figure 1.

Item	Comment	Manufacturer	Article number
Ismatec REGLO ICC digital peristaltic pump; 4-channel, 8-roller		Ismatec	ISM4408
Pump tubing, PharMed® Ismaprene, 1.6 mm inner diameter, 4.8 mm outer diameter, 1.6 mm wall thickness		Ismatec	MF0010
2-stop tubing, PharMed® Ismaprene, 1.65 mm inner diameter		Ismatec	SC0331
In-line stainless steel filter holder, 47 mm		Sartorius	16254
Luer lock connector for filter holders		Sartorius	16881
Whatman® Nuclepore™ Track-Etched Membranes; 47 mm diameter, 0.2 µm pore size, polycarbonate		Whatman	WHA111106
Advantec Grade GC50 Glass Fiber Filters, 47 mm diameter, 0.5 µm pore size	Support filter for E1	Advantec	GC5047MM
GVS Life Sciences Magna™ Nylon Membrane Filters, 47 mm diameter, 0.5 µm pore size	Support filter for E2, Nylon provides a smoother filter surface than the glass fibre support filters used for E1	GVS	1213776
Glass bottle, 1.5 cm inner diameter, 10 cm height, GL25 thread	Medium reservoir for recirculated incubations; custom-made		

280

281 **Table S2.** Test of statistical significance of differences in ^{13}C-enrichment between microbial groups

282 within each approach and differences between approaches within each microbial group. Shown are

283 results of Kruskal-Wallis test and non-parametric multiple comparison test (Dunn's test, see pairwise

284 comparisons column); *P < 0.05, **P < 0.01, ***P < 0.001, n.s. not significant.

		Kruskal-Wallis Test			Dunn's Test, pairwise comparison		
Within approach		**χ2**	**df**	**P-value**	**AOB – NOB**	**NOB – other cells**	**AOB – other cells**
E1	Batch	182.6	2	< 0.001	***	***	***
	Recirculated	134.7	2	< 0.001	***	***	***
	Flow-through	65.1	2	< 0.001	***	n.s.	***
E2	Batch	185.4	2	< 0.001	***	***	***
	Recirculated	193.8	2	< 0.001	***	***	***
	Flow-through	327.6	2	< 0.001	***	n.s.	***

Within microbial group		**χ2**	**df**	**P-value**	**Pairwise comparison**		
					Batch – Recirc.	**Recirc. – Flow-thr.**	**Batch – Flow-thr.**
E1	AOB	157.0	2	< 0.001	***	*	***
	NOB	184.5	2	< 0.001	***	***	***
	Other cells	7.9	2	0.019	*	*	n.s.
E2	AOB	375.0	2	< 0.001	***	***	***
	NOB	98.2	2	< 0.001		***	***
	Other cells	20.3	2	< 0.001	***	***	n.s.

285